Available online at www.sciencedirect.com
ScienceDirect
Cement and Concrete Research 38 (2008) 68–76
Cement and Concrete Research

Effect of limestone filler on the deterioration of mortars and pastes exposed to sulfate solutions at ambient temperature

Seung Tae Lee [a,*], Robert Doug. Hooton [b], Ho-Seop Jung [c], Du-Hee Park [d], Chang Sik Choi [e]

[a] Department of Civil Engineering, Kunsan National University, San 68, Miryong-dong, Kunsan, Jeollabuk-do, 573-701, South Korea
[b] Department of Civil Engineering, University of Toronto, 35 St. George Street, Toronto, ON, Canada M5S 1A4
[c] Korea Institute of Construction Technology, 2311 Daewha-dong, Ilsan-gu, Goyang, Kyeonggi-do, 411-712, South Korea
[d] Department of Civil Engineering, Hanyang University, 17 Haengdang-dong, Seongdong-gu, Seoul, 133-791, South Korea
[e] Division of Architectural Engineering, Hanyang University, 17 Haengdang-dong, Seongdong-gu, Seoul, 133-791, South Korea

Received 29 September 2005; accepted 13 August 2007

Abstract

This paper presents data on engineering properties such as compressive strength, visual change and expansion of mortar specimens incorporating limestone filler subjected to severe sulfate attack at ambient temperature. Specimens with four replacement levels of limestone filler (0, 10, 20 and 30% of cement by mass) were immersed in sodium and magnesium sulfate solutions with 33,800 ppm of SO_4^{2-} concentration. In order to identify the products formed by sulfate attack, microstructural analyses such as XRD and SEM were also performed on the paste samples with similar replacement levels of limestone filler.

The test results demonstrated that mortar and paste samples incorporating higher replacement levels of limestone filler were more susceptible to sulfate attack irrespective of types of attacking sources. However, the deterioration modes were significantly dependent on the types of sulfate solutions. Additionally, although the samples were exposed to sulfate solutions at 20±1 °C, the deterioration was strongly associated with thaumasite formation in both sulfate solutions.

The deterioration mechanism and resistance to sulfate attack of cement matrix incorporating limestone filler at ambient temperature is discussed in the light of the test results obtained.

Keywords: Sulfate attack; Limestone filler; Thaumasite; Sodium sulfate; Magnesium sulfate

1. Introduction

Limestone has been increasingly used in concrete as a filler or as a main cement constituent for many years [1]. It is applied in high performance concrete as well as in normal or low performance concrete [2–4]. Studies related to the mechanical properties of concrete incorporating limestone were carried out to achieve the reliability for increasing usage of limestone filler or cement [3,5]. Moreover, there have been numerous studies on durability of limestone concrete when exposed to aggressive conditions. Most of these studies were focused on the effects of limestone on concrete durability.

In particular, it has been reported that the usage of large volumes of limestone filler in concrete may lead to the increased probability of sulfate attack, associated with thaumasite formation. Commonly, thaumasite forms in the system when concrete incorporating limestone is subjected to sulfate attack typically to low temperature (<5 °C) in an environment with high humidity [6–8]. Many researchers have also tried to reveal the mechanism of thaumasite sulfate attack in paste, mortar or concrete both in the field [9–13] and in the laboratory [6,14–17]. However, recent studies have reported that thaumasite can form at room temperature [15,16,18–20]. Although minor thaumasite formation is not always associated with thaumasite sulfate attack (TSA), TSA can be affected by the type of cations accompanying the SO_4^{2-} ion and the concentration of sulfate solutions [6]. The effect of replacement level of limestone filler on the sulfate deterioration of mortars was also reported [21].

* Corresponding author. Tel.: +82 63 469 4877; fax: +82 63 469 4791.
E-mail address: stlee@kunsan.ac.kr (S.T. Lee).

0008-8846/$ - see front matter © 2007 Elsevier Ltd. All rights reserved.
doi:10.1016/j.cemconres.2007.08.003

Table 1
Chemical composition and physical data for the cement and limestone filler

Chemical composition	Cement[1]	Limestone[2]
SiO_2, %	21.7	0.51
Al_2O_3, %	5.7	0.22
Fe_2O_3, %	3.2	0.09
CaO, %	63.1	54.4
MgO, %	2.8	0.62
SO_3, %	2.2	–
LOI, %	1.3	43.44
Mineralogical compound (Bogue calculation)		
C_2S, %	20.8	–
C_3S, %	42.8	–
C_3A, %	9.7	–
C_4AF, %	9.7	–
Mean diameter, mm	–	3.11
Moisture content, %	–	0.05
Whiteness, %	–	96.5
Specific gravity	3.15	2.71
Fineness, m^2/kg	328	2650

Data were supplied from the manufactures: 1. S cement company Ltd., 2. W Chemicals Ltd.

In the present study, thus, the effect of replacement levels (0, 10, 20 and 30% by mass) of limestone filler on sodium and magnesium sulfate attack at ambient temperature was investigated. The experimental study was developed to obtain conclusive data on negative or positive effects of limestone filler in both sulfate solutions.

2. Experimental procedure

The experimental study was carried out on mortar and paste specimens with or without limestone filler. ASTM C 150 Type I Portland cement was used as binder in all the mortar and paste mixtures. The specific gravity and specific surface area of the cement were 3.15 and 328 m^2/kg, respectively. The chemical composition and mineralogical compounds of the cement are presented in Table 1. Four replacement levels (0, 10, 20, and 30% by mass) of limestone filler as a partial replacement of the cement were chosen as the main variable. The limestone fillers were produced by a company in South Korea. The chemical composition and physical properties from the supplier are also presented in Table 1.

River sand, with a maximum size of 5 mm, was used as the fine aggregate in the mortar mixtures. The physical properties and grading of fine aggregate are indicated in Table 2. The sand/cementitious material ratio and water/cementitious material ratio (w/cm) were fixed at 2.0 and 0.45, respectively, in all the mortar mixtures.

A polycarbonic acid-based superplasticizer was added at the time of mixing to impart good workability to all the mortar mixtures. It was added to the mixing water as 1.8% of mass of cementitious materials.

Table 3
Details of mortar and paste mixtures

Code	Cementitious materials	w/cm
LS0	100% cement	0.45
LS10	90% cement+10% limestone filler	0.45
LS20	80% cement+20% limestone filler	0.45
LS30	70% cement+30% limestone filler	0.45

Mortar and paste specimens were demoulded 24 h after casting, and cured in tap water at room temperature for an additional 6 days. Thereafter some of the specimens were transferred to the sulfate solutions. The temperature of tap water and sulfate solutions was maintained at 20±1 °C during the test period. Table 3 shows the details of the mortar and paste mixtures used in the tests.

Solution concentration was determined at 33,800 ppm as SO_4^{2-} for both sodium and magnesium sulfate solutions. The solutions were refreshed every four weeks up to 1 year.

Compressive strength tests were carried out on 50 mm cube mortar specimens, and performed after 0, 91, 180, 240 and 360 days of sulfate exposure. Strength loss was also investigated by comparing with the compressive strength of mortar specimens cured in tap water. Before testing for compressive strength of cube mortar specimens exposed to sulfate solutions, each specimen was carefully examined to check any surface damage due to sulfate attack. All significant changes at the surface of the specimens were recorded.

Expansion tests on prism mortar specimens (25×25×285 mm), based on ASTM C 1012, were also carried out.

Microstructural observations such as XRD and SEM were performed on paste samples exposed to both sulfate solutions. XRD was conducted using the RINT D/max 2500 (Rigaku, Japan) X-ray diffractometer. For the XRD tests, CuKα radiation with a wavelength of 1.5405 Å at a voltage of 30 kV, scanning speed of 2°/min. and current of 30 mA were used. The microstructure of the paste samples was investigated using an XL30ESEM equipped with EDXA Falcon Energy System 60SEM. The fractured surface samples were obtained from the deteriorated part of the paste specimens. For the investigation by SEM and EDS, the samples were dried in a desiccator for 24 h, and subsequently gold coated.

3. Results

3.1. Compressive strength of mortars

The results for compressive strength development of 50 mm cube specimens with a w/cm of 0.45 cured in tap water at the

Table 2
Physical data and sieve analysis for the fine aggregate used in this study

Specific gravity	Absorption, %	F. M.	Percentage of mass passing through sieve, %					
			5 mm	2.5 mm	1.2 mm	0.6 mm	0.3 mm	150 mm
2.60	0.80	2.80	100	86	68	46	18	2

Table 4
Compressive strength values of mortar specimens cured in tap water

	Compressive strength, MPa		
	3 days	7 days	28 days
LS0	29.9	41.9	49.7
LS10	27.6	38.4	46.8
LS20	23.0	32.5	41.1
LS30	19.9	27.7	36.2

ages of 3, 7 and 28 days are summarized in Table 4. These results clearly show the decreased values of compressive strength with the increased replacement levels of limestone filler. It is believed that these are also partially associated with the change of water to Portland cement ratio with respect to the hydration process.

After the pre-curing for 7 days, in order to characterize the change of compressive strength of mortar specimens incorporating limestone filler due to sulfate attack, the compressive strength values after storage in tap water and sulfate solutions were measured up to 1 year of exposure. Fig. 1 shows the compressive strength of control mortar specimens (LS0) without limestone filler under both tap water and sulfate solutions. While the values of compressive strength of the specimens in tap water increased (or stabilized) with time, those of the specimens stored in sodium and magnesium sulfate solutions decreased after an exposure of 91 days. In particular, the mortar specimens exposed to magnesium sulfate solution showed lower compressive strength values compared to those exposed to sodium sulfate solution, irrespective of exposure period [22].

The compressive strength values of mortar specimens with limestone filler of 10, 20 and 30% replacement levels in tap water and sulfate solutions are plotted in Figs. 2, 3 and 4, respectively. Similarly the compressive strength of mortar specimens incorporating limestone filler exposed to sulfate solutions gradually decreased after 91 days. As the replacement level of limestone filler increased, the extent of reduction in compressive strength was more in both sodium and magnesium sulfate solution, as shown in Figs. 2, 3 and 4, respectively. After an exposure of 360 days in sodium sulfate solution, while the compressive strength of LS0 mortar specimen without limestone filler were 44.6 MPa, the LS10, LS20 and LS30 mortar specimens were only 36.2, 25.5 and 15.5 MPa, respectively. Under magnesium sulfate attack, the 1-year compressive strength values of mortar mixtures for LS0, LS10, LS20 and LS30 were 35.3, 24.3, 15.5 and 5.6 MPa, respectively.

Figs. 5 and 6 show the compressive strength of the mortar specimens under sodium and magnesium sulfate attack, relative to the compressive strength of the mortar specimens in tap water. These results also emphasize that the incorporation of limestone filler leads to increased strength loss compared with that of LS0 mortar specimen, regardless of sulfate solutions. Further, it is confirmed that the values of strength loss greatly depend on the replacement levels of limestone filler, especially at later exposure periods.

These results imply the negative effect of limestone filler on the characteristic of compressive strength of mortar specimen under sulfate attack orienting from sodium and magnesium sulfate solutions, and are in agreement with those reported elsewhere [21,23].

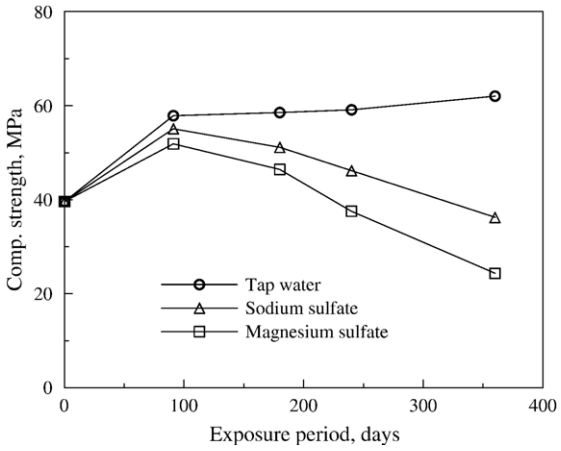

Fig. 2. Compressive strength of LS10 mortar specimens.

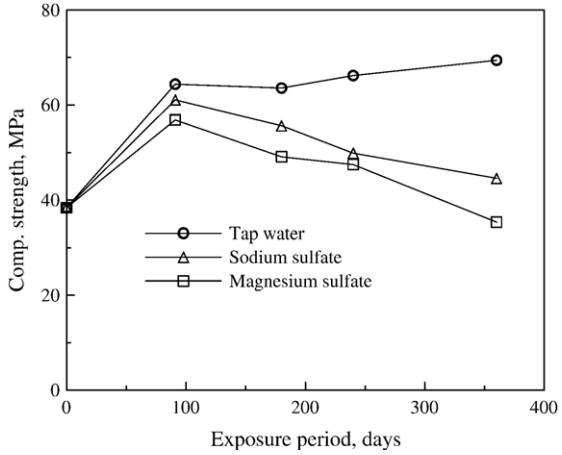

Fig. 1. Compressive strength of LS0 mortar specimens.

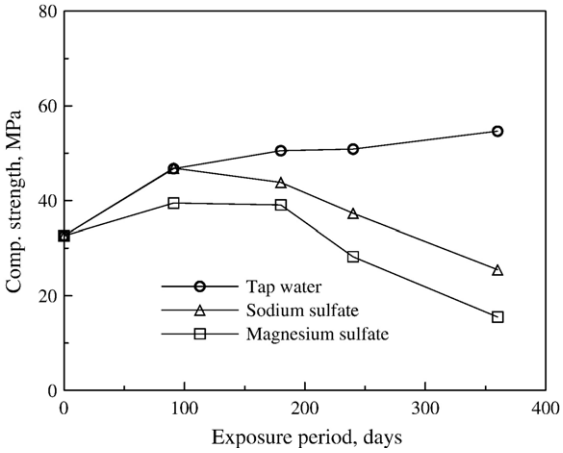

Fig. 3. Compressive strength of LS20 mortar specimens.

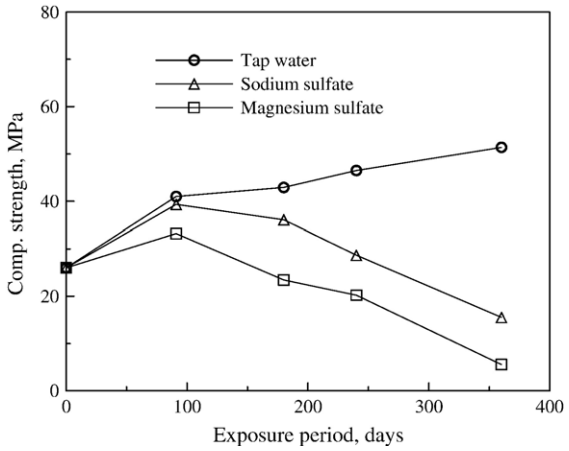

Fig. 4. Compressive strength of LS30 mortar specimens.

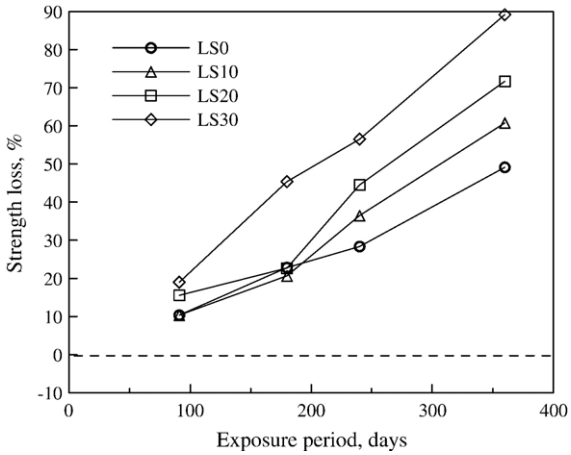

Fig. 6. Strength loss of mortar specimens exposed to magnesium sulfate solution.

3.2. Visual inspection of mortars

A visual inspection was carried out to evaluate the visible signs of surface deterioration such as spalling, cracking and softening in mortar specimens exposed to sulfate attack.

Figs. 7 and 8 show examples of surface deterioration of mortar cubes exposed to sulfate attack after 360 days of immersion in both sulfate solutions. Regardless of exposure solutions and replacement levels of limestone filler, the first sign of sulfate attack was the deterioration of the corners of the mortar samples followed by damage at the edges and the faces.

In sodium sulfate solution, it is clearly observed that the degree of surface deterioration is different with the replacement levels of limestone filler as shown in Fig. 7. The extent of surface deterioration after 360 days of exposure has a tendency to increase with the increased replacement level of limestone filler. In other words, the LS30 mortar sample displayed many wide cracks, spalling and substantial material loss at the faces as well as at the corners and edges, while the LS0 mortar sample only exhibited cracks around corners and edges.

In magnesium sulfate solution, as shown in Fig. 8, the negative effect of the higher replacement level of limestone filler was observed more remarkably. While slight spalling was observed at the corners of the LS0 mortar sample, the LS30 mortar sample (Fig. 8(d)) showed severe surface deterioration like onion skin peeling due to the extensive spalling and cracking at all the surfaces of the specimen. The results of visual inspection are in good agreement with those of compressive strength and strength loss shown in Figs. 1–6. More importantly, it could be concluded that the sulfate deterioration modes of mortar specimen incorporating limestone filler are greatly associated with the types of exposure solutions.

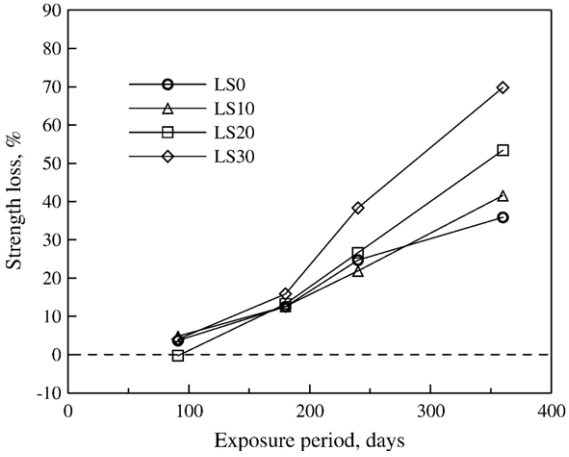

Fig. 5. Strength loss of mortar specimens exposed to sodium sulfate solution.

3.3. Expansion of mortars

The expansion data of mortar specimens incorporating limestone filler are summarized in Tables 5 and 6, respectively. The expansion values presented in Table 5 relate to mortar specimens with partially replaced limestone filler at replacement levels of 0, 10, 20 and 30% under sodium sulfate environment. The results indicate a significant increase in expansion of the mortar specimens with increased replacement levels of limestone filler. For LS0 mortar specimens without limestone filler, the expansion values were relatively low compared with those of mortar specimens incorporating limestone filler. As well, LS20 and LS30 mortar specimens, which had limestone filler of 20 and 30% replacement level of cement by mass, were disintegrated after 360 days of exposure.

The expansion data also indicate that the expansion of mortar specimens exposed to sodium sulfate solution was higher than those of mortar specimens exposed to magnesium sulfate solution with similar solution concentration of sulfate ions. This may be due to the difference in stability of sulfate products formed between sodium and magnesium sulfate attack [22].

3.4. Microstructural observations of pastes

XRD and SEM observations on paste samples with or without limestone filler were carried out to identify the products formed by sulfate attack.

Fig. 7. Cube mortar specimens exposed to sodium sulfate solution (360 days).

Paste specimens incorporating limestone filler were examined by XRD after 360 days of immersion in sodium and magnesium sulfate solution at 20±1 °C. Fig. 9 shows the XRD patterns for the powdered samples from the paste specimens exposed to sodium sulfate solution. As expected, the relatively strong calcite peaks were detected in LS10, LS20 and LS30 paste samples due to the replacement of cement by limestone filler. The peak intensities for portlandite were observed in XRD patterns for all paste samples, and their relative intensity is largely dependent on the replacement level of limestone filler.

Another important observation is the absence or negligible level of gypsum formation in the XRD traces for LS20 and LS30 paste samples, while the XRD pattern for the LS0 paste sample showed relatively strong intensity peaks for gypsum formation at around 11.7 and 20.7° 2θ. For the LS30 paste samples, the thaumasite peaks were very intense compared with those in the LS0 paste sample. This suggests that, in case of cement systems incorporating high levels of limestone filler under sodium sulfate environment, one of primary causes for sulfate damage may be thaumasite formation, but not gypsum formation.

Compared with the XRD results of paste samples exposed to sodium sulfate solution, a different trend on gypsum formation is present in XRD patterns of the powdered samples drawn from paste specimens exposed to magnesium sulfate solution, as shown in Fig. 10. After the exposure of 360 days, the gypsum peaks were very strong, especially in the LS30 paste sample, compared with peaks of other products formed. Additionally, there were very weak peaks for portlandite in XRD patterns of the LS20 and LS30 paste samples. This indicates that the samples were suffering severely from magnesium sulfate attack. Also, it was observed that the intensity of peaks for thaumasite at around 9.1 and 16.0° 2θ increased with the increased replacement levels of limestone filler. It was, therefore, found that the peak intensity of gypsum and thaumasite has a good relationship with surface damage by magnesium sulfate attack, as already shown in Fig. 8.

SEM observations were used to identify products formed by sulfate attack. Examined samples had been immersed in sodium or magnesium sulfate solution for 360 days.

Fig. 11 shows the SEM image on the surface of the LS30 paste sample exposed to sodium sulfate solution and indicates the presence of numerous crystals. Examination at higher magnification was performed on the open square in the image as presented in Fig. 12. It was observed that the crystals were very fine (below 0.5 μm in thickness) and up to 10 μm in length. EDS analysis indicated, as shown in Fig. 12, that these crystals consist of the elements of calcium, sulfur, oxygen, aluminum, silicon as well as a small amount of carbon. This suggests that there was a possible presence of a mixture of thaumasite and ettringite in the paste sample exposed to sodium sulfate solution. Similar to the XRD results, there was no evidence of the presence of gypsum on the surface of the sample by SEM and EDS analysis.

Fig. 13 shows SEM image on the surface region of the LS30 paste after immersion in magnesium sulfate solution. As expected, it was found that a layer of brucite had developed in the system. Further investigation around a crack, which can be seen in the center of the image, at higher magnification was carried out, as shown in Fig. 14 and obviously indicated the presence of gypsum and thaumasite as confirmed by EDS

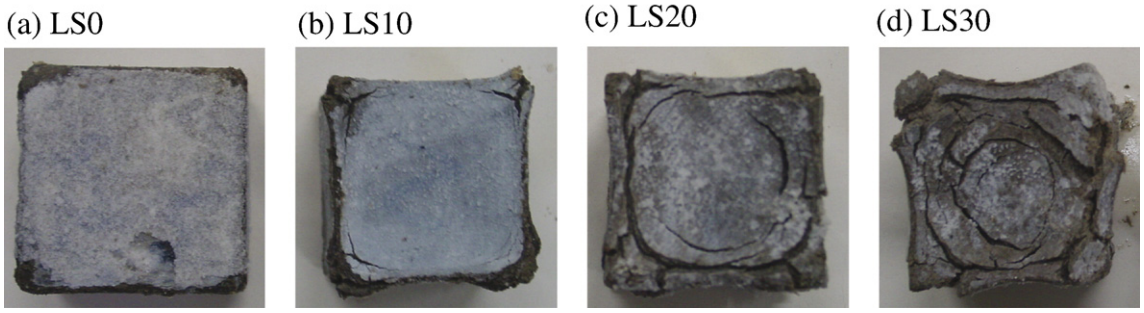

Fig. 8. Cube mortar specimens exposed to magnesium sulfate solution (360 days).

Table 5
Expansion of mortar specimens exposed to sodium sulfate solution

Exposure period, days	Expansion, %			
	LS0	LS10	LS20	LS30
180	0.086	0.057	0.291	0.414
240	0.261	0.274	0.595	0.692
360	0.446	0.549	Disintegration	Disintegration

analysis. It was found that the tabular gypsum crystals were surrounded by a mass of clusters of thaumasite [16].

4. Discussion

Sulfate attack has often been discussed in terms of the reaction between the cement hydrates and dissolved compounds in the attacking solution [24]. There have been many studies related to sulfate deterioration products such as ettringite, gypsum, M–S–H and brucite in the field of sulfate attack [24–26]. Moreover, as stated earlier, many researchers [1,8,18,20,21] have reported that the sulfate deterioration in cement system incorporating significant levels of limestone filler at ambient temperature as well as low temperature is associated with the formation of thaumasite. It must be noted that this has not been found for the 3–5% levels of limestone commonly added to many Portland cements. Adversely, Torres et al. [17] have reported that the thaumasite was formed in cement mortars containing 5% limestone replacement, as well as in a higher replacement of limestone (15 to 30%), especially when those mortars were exposed to magnesium sulfate solution at a low temperature (5 °C).

Generally in order to form thaumasite, decomposition of C–S–H by sulfate attack could be the source of silica available in pore solution that reacts with the calcium carbonate from limestone filler [18].

The overall aim of the present study is to establish the material durability of mortar and paste specimens incorporating limestone filler form 10% up to 30% of cement by mass, particularly when they are continually exposed to severe sulfate environments at ambient temperature.

The one year data on compressive strength, visual inspection and expansion described above make it clear that the use of limestone filler in the cement system leads to a poor resistance to both sodium and magnesium sulfate attack. Furthermore, higher replacement levels showed substantial strength loss and expansion on mortar specimens exposed to sulfate environments when compared with the performance of the control mortar specimen without limestone filler.

Table 6
Expansion of mortar specimens exposed to magnesium sulfate solution

Exposure period, days	Expansion, %			
	LS0	LS10	LS20	LS30
180	0.056	0.064	0.164	0.220
240	0.072	0.205	0.321	0.468
360	0.244	0.332	Disintegration	Disintegration

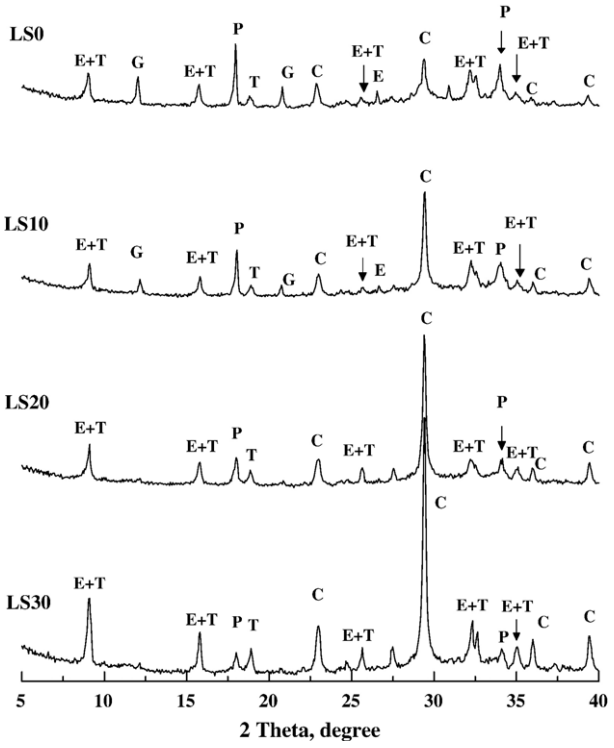

Fig. 9. XRD patterns of paste samples exposed to sodium sulfate solution for 360 days (note: E = ettringite, T = thaumasite, P = portlandite, G = gypsum, C = calcite).

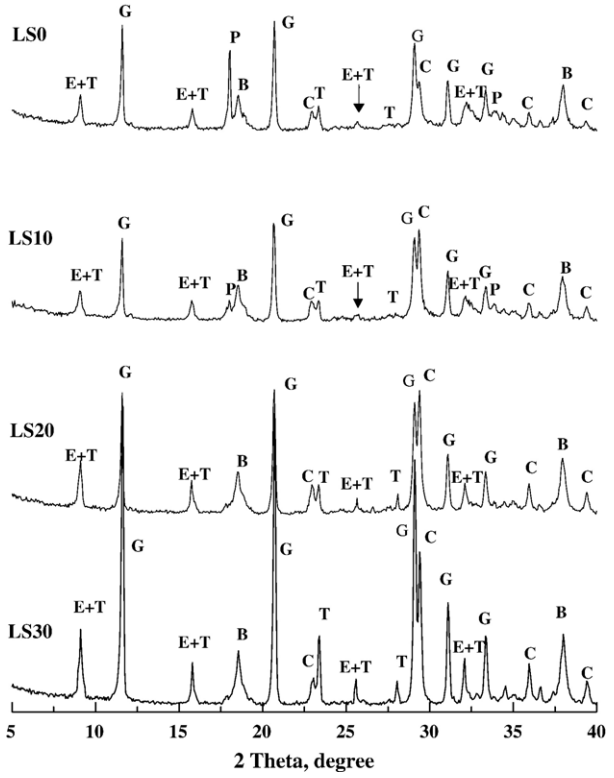

Fig. 10. XRD patterns of paste samples exposed to magnesium sulfate solution for 360 days (note: E = ettringite, T = thaumasite, P = portlandite, C = calcite, G = gypsum, B = brucite).

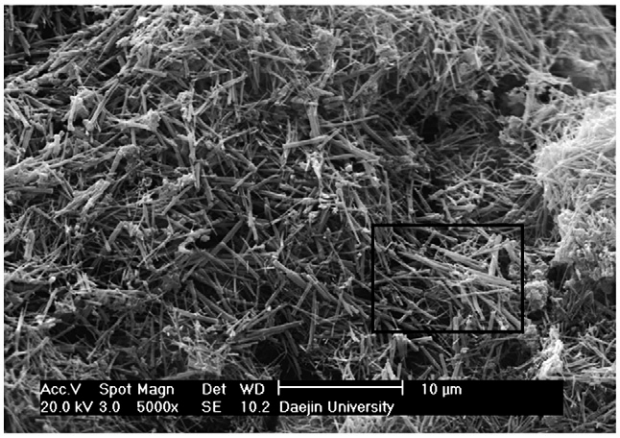

Fig. 11. SEM image of LS30 paste sample exposed to sodium sulfate solution for 360 days (ettringite + thaumasite).

The compressive strength data shown in Figs. 1–4 emphasize the more pronounced negative effect of magnesium sulfate attack compared to that of sodium sulfate attack in mortar systems incorporating limestone filler. The results of strength loss (Figs. 5 and 6) clearly support this trend. Moreover, mineralogical

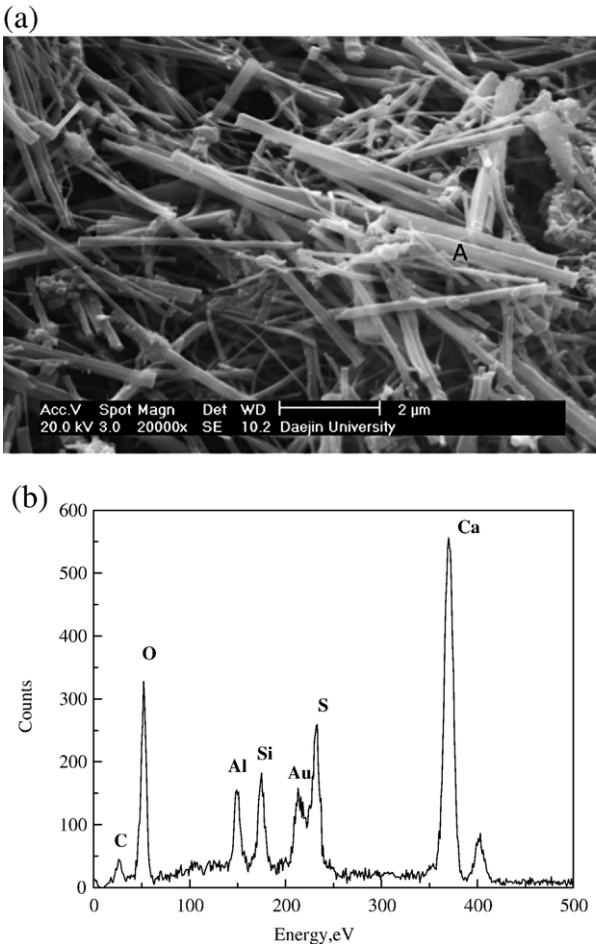

Fig. 12. SEM image (higher magnification of Fig. 11) and EDS profile (A) of LS30 paste sample exposed to sodium sulfate solution for 360 days.

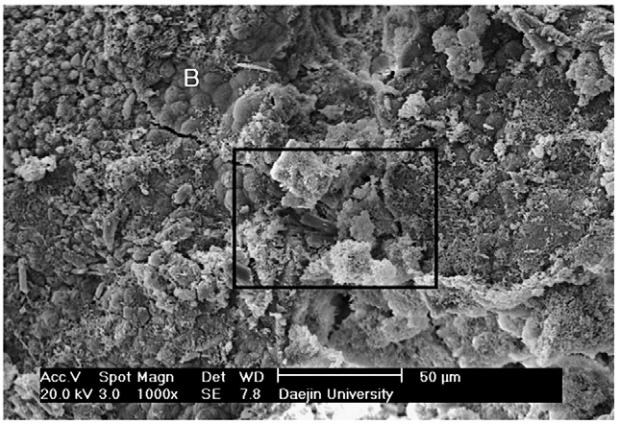

Fig. 13. SEM image of LS30 paste sample exposed to magnesium sulfate solution for 360 days (B: brucite).

analyses based on XRD suggest that the primary cause for deterioration due to magnesium sulfate attack may be attributed to gypsum formation as well as thaumasite formation. These results are in agreement with those reported by Hartshorn et al. [16] which showed that the formation of gypsum and thaumasite play a dominant role in aggravating cement systems with limestone filler due to magnesium sulfate attack.

Generally, it has been reported that the presence of thaumasite is often preceded by the formation of ettringite [20]. However, although the final stage of deterioration in cement system is characterized by the presence of thaumasite, especially in the outer surface, it should also be noted that there is a possibility of co-existence of thaumasite and ettringite due to solid-solution effect. In other words, the conversion of both phases can be occurred in the region related to ingress of sulfate ions induced from external sulfate sources.

With respect to the strength loss of mortar specimens, the worst performance was observed in the LS30 mortar specimen exposed to magnesium sulfate solution compared to same mortar specimen exposed to sodium sulfate solution. However, sodium sulfate attack led to more expansion in mortar specimens than magnesium sulfate attack. These phenomena are largely related to the kinds of products formed by sulfate attack.

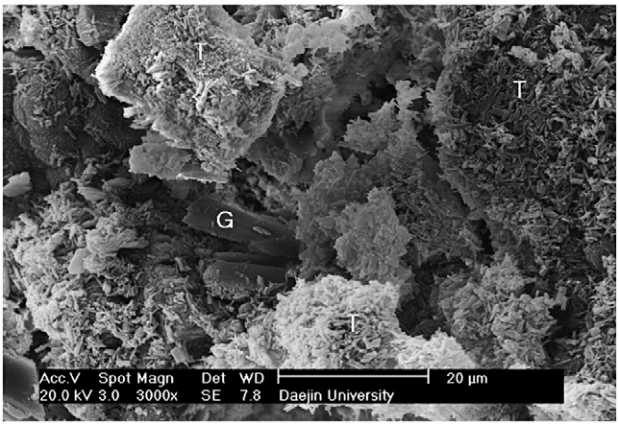

Fig. 14. SEM image of LS30 paste sample exposed to magnesium sulfate solution for 360 days (G: gypsum, T: thaumasite).

Under magnesium sulfate attack, decalcification of C–S–H, which results from the progressive decrease in C/S ratio within the C–S–H, contributes to pH drops to low levels (<10) [28]. Even if ettringite succeeds in forming during magnesium sulfate attack, the product is prone to be unstable in the low alkalinity provided by the brucite formation [22]. On the contrary, in case of sodium sulfate attack, the sodium hydroxide formed compensates for the loss of alkalinity caused by the consumption of calcium hydroxide. Ettringite formed can be stable, and finally leads to an excessive expansion in the cement matrix. Moreover, it has been reported in the literature [26,27,29] that gypsum rather than ettringite would tend to form in magnesium sulfate environment because of locally reduced pH and the limited local availability of aluminum. Recently, however, some researchers suggested the possibility of expansion due to gypsum formation [19,30]. In the present study, it is thought that a great amount of the gypsum formation in LS20 and LS30 prism mortar specimens may be partly responsible for the disintegration in magnesium sulfate solution after 1 year of exposure (Tables 5 and 6). However, the possibility of expansion due to thaumasite formation is still unclear.

It was found that there was an excellent correspondence between mechanical properties and visible damage on surfaces of mortar specimens exposed to sulfate solutions. However, deterioration modes of the mortar specimens were dependent on the attacking sources. In other words, while sodium sulfate attack causes the surface damage, showing wide cracks due to expansion, softening and delamination are the primary deterioration phenomena for the mortar specimen exposed to magnesium sulfate attack [29].

XRD analyses presented in Figs. 9 and 10 indicate that cement matrices with limestone filler under magnesium sulfate attack behave very differently from those exposed to sodium sulfate attack with respect to the mode of deterioration. More importantly, the peaks for gypsum are absent or negligible in the paste samples with higher replacement levels of limestone filler (LS20 and LS30) exposed to sodium sulfate solution.

5. Conclusions

In this study, the test results emphasized the negative effect of 10 to 30% limestone filler replacement of non-sulfate resistant Type I cement on the resistance of mortar specimens when they are subject to sodium and magnesium sulfate attack at ambient temperature. Especially it was clearly observed from the visual inspection that the mortar specimens with higher replacement levels of limestone filler suffered more pronounced deterioration in both sulfate solutions, when compared to those without limestone filler. Additionally, based on XRD analysis, it was confirmed that the main cause of deterioration for the LS30 paste sample exposed to sodium sulfate solution is thaumasite formation. On the contrary, gypsum formation as well as thaumasite formation is primarily responsible for the deterioration of cement systems incorporating higher replacement levels of limestone filler under magnesium sulfate attack.

However, it should be noted that all specimens used in this study were tested after curing and exposure at an environment of around 20±1 °C. Comparison with the test results performed at low temperature should be considered. It should also be noted that the Portland cement used was not sulfate resistant, and no tests were performed using the 3 to 5% limestone levels commonly found in Portland cements.

Acknowledgements

This work was supported by Sustainable Building Research Center of Hanyang University which was supported the SRC/ERC program of MOST (grant R11-2005-056-030020-0) and the search fund of the CCTRD of MOCT (grant C105A1050001-05A0505-00210).

References

[1] S. Tsivilis, G. Kakali, A. Skaropoulou, J.H. Sharp, R.N. Swamy, Use of mineral admixtures to prevent thaumasite formation in limestone cement mortar, Cem. Concr. Compos. 25 (8) (2003) 969–976.
[2] L. Svermova, M. Sonebi, P.J.M. Bartos, Influence of mix proportions on rheology of cement grouts containing limestone powder, Cem. Concr. Compos. 25 (7) (2003) 737–749.
[3] A. Yahia, M. Tanimura, Y. Shimoyama, Rheological properties of highly flowable mortar containing limestone filler-effect of powder content and W/C ratio, Cem. Concr. Res. 35 (3) (2005) 532–539.
[4] N. Voglis, G. Kakali, E. Chaniotakis, S. Tsivilis, Portland-limestone cements. Their properties and hydration compared to those of other composite cements, Cem. Concr. Compos. 27 (2) (2005) 191–196.
[5] S. Tsivilis, J. Tsantilas, G. Kakali, E. Chaniotakis, A. Sakellariou, The permeability of Portland limestone cement concrete, Cem. Concr. Res. 33 (9) (2003) 1465–1471.
[6] S.A. Hartshorn, J.H. Sharp, R.N. Swamy, Thaumasite formation in Portland-limestone cement pastes, Cem. Concr. Res. 29 (8) (1999) 1331–1340.
[7] N.J. Crammond, M.A. Halliwell, Assessment of the conditions required for the thaumasite form of sulfate attack, in: K.L. Scrivener, J.F. Young (Eds.), Mechanisms of chemical Degradation of Cement Based System, E&FN Spon, London, 1997, pp. 193–200.
[8] T. Vuk, R. Gabrovsek, V. Kaucic, The influence of mineral admixtures on sulfate resistance of limestone cement pastes aged in cold $MgSO_4$ solution, Cem. Concr. Res. 32 (6) (2002) 943–948.
[9] M. Collepardi, Degradation and restoration of masonry walls of historical buildings, Mater. Struct. 23 (1990) 81–102.
[10] S. Sahu, S. Badger, N. Thaulow, Evidence of thaumasite formation in Southern California concrete, Cem. Concr. Compos. 24 (3) (2002) 379–384.
[11] J.A. Bickley, R.T. Hemmings, R.D. Hooton, J. Balinski, Thaumasite related deterioration of concrete structures, Am. Concr. Inst. SP-144 (1994) 159–175.
[12] N. Crammond, The occurrence of thaumasite in modern construction — a review, Cem. Concr. Compos. 24 (3) (2002) 393–402.
[13] S. Diamond, Thaumasite in Orange Country, Southern California: an inquiry into the effect of low temperature, Cem. Concr. Compos. 25 (8) (2003) 1161–1164.
[14] K.N. Jallad, M. Santhanam, M.D. Cohen, Stability and reactivity of thaumasite at different pH levels, Cem. Concr. Res. 33 (3) (2003) 433–437.
[15] P. Brown, R.D. Hooton, Ettringite and thaumasite formation in laboratory concretes prepared using sulfate-resisting cements, Cem. Concr. Compos. 24 (3) (2002) 361–370.
[16] S.A. Hartshorn, J.H. Sharp, R.N. Swamy, The thaumasite form of sulfate attack in Portland-limestone cement mortars stored in magnesium sulfate solution, Cem. Concr. Compos. 24 (3) (2002) 351–359.
[17] S.M. Torres, J.H. Sharp, R.N. Swamy, C.J. Lynsdale, S.A. Huntley, Long term durability of Portland-limestone cement mortars exposed to magnesium sulfate attack, Cem. Concr. Compos. 25 (8) (2003) 947–954.

[18] E.F. Irassar, V.L. Bonavetti, M.A. Trezza, M.A. Gonzalez, Thaumasite formation in limestone filler cements exposed to sodium sulphate solution at 20 °C, Cem. Concr. Compos. 27 (1) (2005) 77–84.
[19] M. Santhanam, M.D. Cohen, J. Olek, Effects of gypsum formation on the performance of cement mortars during external sulfate attack, Cem. Concr. Res. 33 (3) (2003) 325–332.
[20] E.F. Irassar, V.L. Bonavetti, M. Gonzalez, Microstructural study of sulfate attack on ordinary and limestone Portland cements at ambient temperature, Cem. Concr. Res. 33 (1) (2003) 31–41.
[21] S.A. Hartshorn, R.N. Swamy, J.H. Sharp, Engineering properties and structural implications of Portland limestone cement mortar exposed to magnesium sulphate attack, Adv. Cem. Res 13 (1) (2001) 31–46.
[22] O.S.B. Al-Amoudi, M. Maslehuddin, M.M. Saadi, Effect of magnesium sulfate and sodium sulfate on the durability performance of plain and blended cements, ACI Mater. J. 92 (1) (1995) 15–24.
[23] H. Justnes, Thaumasite formed by sulfate attack on mortar with limestone filler, Cem. Concr. Compos. 25 (8) (2003) 955–959.
[24] H.F.W. Taylor, Cement Chemistry, 2nd ed., Thomas Telford, London, 1997.
[25] H.Y. Moon, S.T. Lee, S.S. Kim, Sulphate resistance of silica fume blended mortars exposed to various sulphate solutions, Can. J. Civ. Eng. 30 (4) (2003) 625–636.
[26] Rasheeduzzafar, O.S.B. Al-Amoudi, S.N. Abduljauwad, M. Maslehuddin, Magnesium–sodium sulfate attack in plain and blended cements, J. Mater. Civ. Eng. 6 (2) (1994) 201–222.
[27] D.A. Bonen, Microstructural study of the effect produced by magnesium sulfate on plain and silica fume-bearing Portland cement mortars, Cem. Concr. Res. 23 (3) (1993) 541–553.
[28] M. Santhanam, Studies on sulfate attack: mechanism, test methods, and modeling, PhD thesis, Purdue Univ. 2001.
[29] O.S.B. Al-Amoudi, Sulfate attack and reinforcement corrosion in plain and blended cements exposed to sulfate environments, Build. Environ. 33 (1) (1998) 53–61.
[30] B. Tian, M.D. Cohen, Does gypsum formation during sulfate attack on concrete lead to expansion? Cem. Concr. Res. 30 (1) (2000) 117–123.